RESEARCH ARTICLE

Visualization of an Alphaherpesvirus Membrane Protein That Is Essential for Anterograde Axonal Spread of Infection in Neurons

M. P. Taylor, T. Kramer, M. G. Lyman,* R. Kratchmarov, and L. W. Enquist

Department of Molecular Biology, Princeton University, Princeton, New Jersey, USA

* Present address: University Multispectral Laboratories, Ponca City, Oklahoma, USA.

ABSTRACT **Pseudorabies virus (PRV), an alphaherpesvirus with a broad host range, replicates and spreads in chains of synaptically connected neurons. The PRV protein Us9 is a small membrane protein that is highly conserved among alphaherpesviruses and is essential for anterograde axonal spread in neurons. Specifically, the Us9 protein is required for the sorting of newly assembled PRV particles into axons. However, the molecular details underlying the function of Us9 are poorly understood. Here we constructed PRV strains that express functional green fluorescent protein (GFP)-Us9 fusion proteins in order to visualize axonal transport of viral particles in infected rat superior cervical ganglion neurons. We show that GFP-Us9-labeled structures are transported exclusively in the anterograde direction within axons. Additionally, the vast majority of anterograde-directed capsids (labeled with VP26-monomeric red fluorescent protein) and a viral membrane protein (labeled with glycoprotein M fused to mCherry) are cotransported with GFP-Us9 in the anterograde direction. In contrast, during infection with PRV strains that express nonfunctional mutant GFP-Us9 proteins, cotransport of mutant GFP-Us9 with capsids in axons is abolished. These findings show that axonal sorting of progeny viral particles is dependent upon the association of viral structures with membranes that contain functional Us9 proteins. This association is required for anterograde spread of infection in neurons.**

IMPORTANCE **Alphaherpesviruses, such as pseudorabies virus (PRV), are parasites of the mammalian nervous system. These viruses spread over long distances in chains of synaptically connected neurons. PRV encodes several proteins that mediate directed virion transport and spread of infection. Us9 is a highly conserved viral membrane protein that is essential for anterograde neuronal spread of infection. In the absence of Us9, newly replicated viral particles are assembled in the cell body but are not sorted into or transported within axons. Here, we constructed and characterized novel PRV strains that express functional green fluorescent protein (GFP)-Us9 fusion proteins in order to visualize its localization in living neurons during infection. This enabled us to better understand the function of Us9 in facilitating the spread of infection. We show that all viral particles moving in the anterograde direction are labeled with GFP-Us9, suggesting that the presence of Us9 determines the capacity for directed transport within axons.**

Received 2 March 2012 **Accepted** 7 March 2012 **Published** 23 March 2012

Citation Taylor MP, Kramer T, Lyman MG, Kratchmarov R, Enquist LW. 2012. Visualization of an alphaherpesvirus membrane protein that is essential for anterograde axonal spread of infection in neurons. mBio 3(2):e00063-12. doi:10.1128/mBio.00063-12.

Editor Terence Dermody, Vanderbilt University Medical Center

Address correspondence to Lynn W. Enquist, lenquist@princeton.edu.

Alphaherpesviruses, including the human pathogens herpes simplex virus 1 (HSV-1), HSV-2, and varicella-zoster virus, are neuroinvasive pathogens that replicate and spread within the mammalian nervous system (1, 2). In their natural hosts, these viruses enter the peripheral nervous system (PNS) and establish lifelong persistent infections in sensory ganglia. Periodically, newly replicated viral particles are transported out toward the periphery and cause recurrent disease. In rare cases, infection spreads from the PNS to the central nervous system, an event that is often lethal. Spread of infection, both within and between hosts, is integral to the viral life cycle and requires bidirectional transport of viral particles over long distances in axons. Specifically, retrograde axonal transport of viral particles (toward the neuron cell body) is required to initiate infection and establish latency, while anterograde axonal transport (away from the neuron cell body) is required to spread infection to the periphery. The directional spread of viral infection is controlled by the action of specific viral proteins.

Pseudorabies virus (PRV) is an alphaherpesvirus with a broad host range that is used extensively for studying viral spread in the nervous system (3, 4). PRV proteins that are important for anterograde spread of infection include highly conserved glycoprotein I (gI), gE, and Us9 (5–7). Of these three proteins, only PRV Us9 is essential for anterograde spread of infection in neurons both *in vitro* and *in vivo* (5, 8, 9). PRV Us9 is a small (98-amino-acid) type II tail-anchored membrane protein enriched in lipid raft microdomains. These attributes allow Us9 to accumulate in the cellular plasma membrane and trans-Golgi network and incorporate into virion envelopes (5, 10, 11). However, the molecular mechanisms underlying Us9's role in viral spread and directed axonal transport of viral particles remain poorly understood.

Anterograde spread involves the sequential steps of sorting

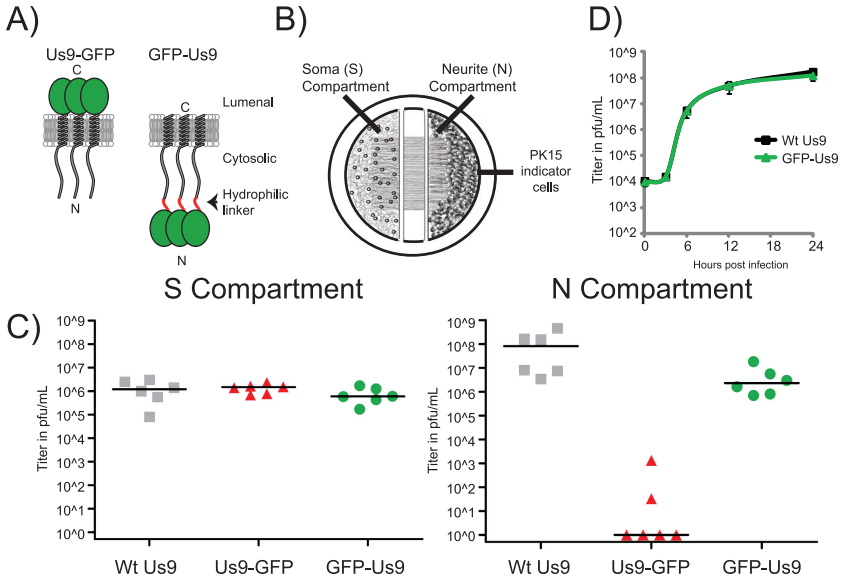

FIG 1 Construction and characterization of the GFP-Us9 fusion. (A) Schematic representations of Us9-GFP and GFP-Us9 enriched in lipid raft microdomains in relation to intracellular membranes. (B) Schematic design of the compartmentalized chamber SCG neuronal culture. Dissociated SCG neurons are seeded into the S compartment. Neurons are cultured for 3 weeks and extend neurites into the N compartment. PK15 cells are seeded into the N compartment 1 day prior to S compartment infection. All cells are harvested by scraping prior to viral titer determination. (C) Viral titers of wild-type (Wt) Us9 (PRV 328), Us9-GFP (PRV 164), and GFP-Us9 (PRV 340) in the S and N compartments of compartmentalized neuronal cultures were determined 24 h postinfection of the S compartment. Titers represent two biological replicates with three chambers for each virus. Median values are plotted as solid lines. (D) Single-step growth curves for wild-type Us9-expressing (PRV 328) or GFP-Us9-expressing (PRV 340) virus on PK15 cells were determined. Cells and medium were harvested at 0, 3, 6, 12, and 24 h after infection at an MOI of 10 PFU per cell.

newly synthesized progeny virions to the axon, long-distance transport within axons, and subsequent egress and entry into a susceptible cell. The assembly state of the transported virion moving in the anterograde direction has been highly contested. Evidence that fully assembled, mature PRV particles undergo anterograde transport comes from several studies using live-cell imaging of fluorescently tagged PRV mutants replicating in dispersed neuronal cultures or in Campenot chambers coupled with transmission electron microscopy (8, 12–17). Us9 is also predicted to be on the surface of anterograde-directed vesicles containing virions (10, 11, 18). Notably, Us9-null mutants assemble and release virions from the cell body but do not sort or transport these newly synthesized virions into axons.

In this study, we constructed and characterized PRV strains that express a novel green fluorescent protein (GFP) fusion to the amino terminus of Us9 (GFP-Us9). We demonstrate that GFP-Us9 retains the capacity for anterograde-directed spread of PRV. We also generated PRV strains expressing the GFP-Us9 fusion protein or GFP-Us9 missense protein in combination with other fluorescent viral structural proteins. These strains enabled us to visualize the transport dynamics of PRV particles in relation to GFP-Us9 using live-cell imaging. We found that the functional GFP-Us9 fusion protein is associated with nearly all virions moving in the anterograde direction, suggesting that Us9 may directly engage viral or host factors that facilitated axonal sorting and transport of intracellular virions.

RESULTS

Construction and validation of PRV expressing GFP-Us9. In this study, we constructed PRV recombinants that express a GFP fusion to the amino terminus of Us9 (GFP-Us9). These strains retained the capacity to promote the sorting and transport of viral structural proteins into axons. We were guided by previous work with other viral homologs of Us9 which suggested that the amino terminus could accommodate large amino acid additions without compromising anterograde spread function (19). In addition, a carboxy-terminal GFP fusion to Us9 (Us9-GFP) could not promote axonal sorting and anterograde spread of infection *in vitro* or *in vivo* (20). The presence of the bulky GFP on the Us9 carboxy terminus appears to disrupt the sorting and transport of viral structures (20) (Fig. 1A), presumably through interference with protein-protein interactions. To limit steric hindrance at the amino terminus, we added a flexible linker between GFP and Us9 (Fig. 1A). To test whether PRV expressing GFP-Us9 was capable of anterograde spread, we used a well-characterized compartmentalized chamber system adapted by Ch'ng and Enquist (13, 21, 22) (Fig. 1B and Materials and Methods). This system has been used to examine the Us9-mediated anterograde spread of PRV from neuronal cell bodies (soma or S compartment) into susceptible epithelial cells plated on isolated distal axons (neurite or N compartment) (Fig. 1B). The viral titers achieved in the N compartment represent a measure of axonal anterograde spread to, and amplification by, epithelial PK15 cells. Wild-type virus infections typically spread to the N compartment via axonal transport and reach a maximum titer within 24 h of S compartment infection. In contrast, chamber infection with PRV strains that do not express Us9 or express a nonfunctional mutant Us9 protein results in essentially no infectious virus in the N compartment (8, 18–20).

The S compartments of compartmentalized neuronal cultures were infected with PRV strains expressing wild-type Us9 (PRV 328) (20), Us9-GFP (PRV 164) (20), or GFP-Us9 (PRV 340) (this study). At 24 h postinfection, viral titers in the S compartment

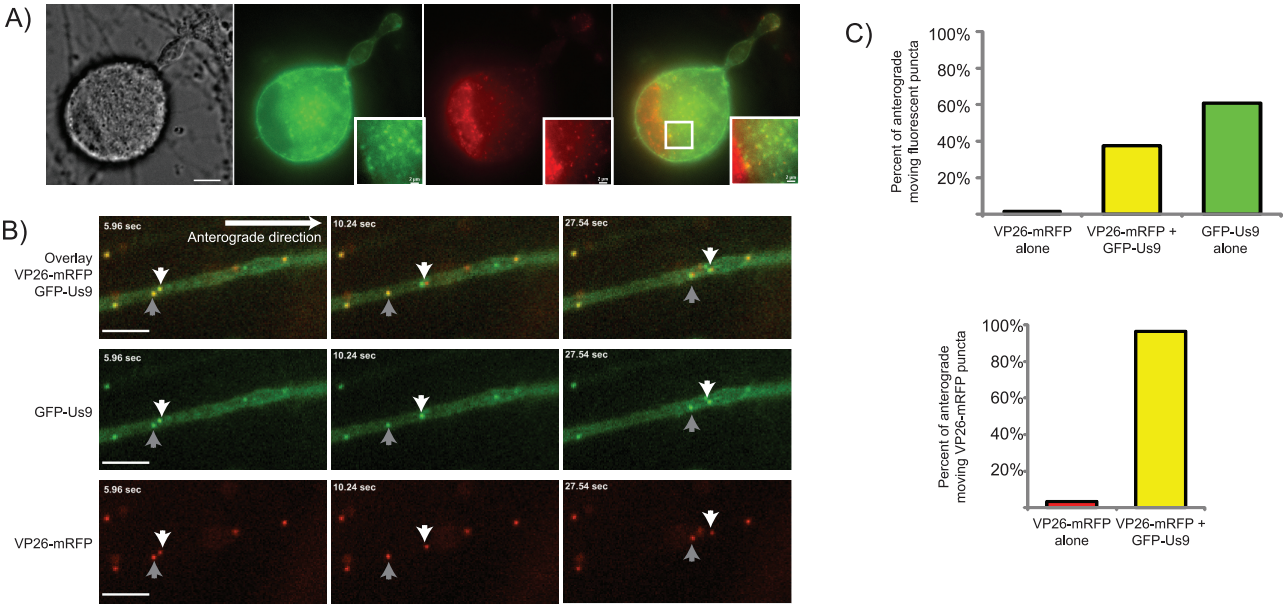

FIG 2 Subcellular localization of GFP-Us9 in PRV-infected SCG neurons. (A) An SCG cell body infected with PRV 341 for 18 h. Differential interference contrast and GFP, mRFP, and merged GFP-mRFP fluorescence images are shown. Inset of a region of neuronal cytoplasm (white box in merged image) containing VP26-mRFP and GFP-Us9 puncta. Scale bar, 2 μm. (B) Representative frames from Movie S1 in the supplemental material with GFP-Us9, mRFP-capsid (VP26-mRFP), and an overlay of the two fluorescence channels are displayed as indicated. PRV 341 was used to infect dissociated SCG neurons. Axons at sites distal from the cell body were imaged by epifluorescence microscopy at 8.5 h postinfection. Scale bars, 5 μm. (C) Quantitation of fluorescent puncta from multiple movies with isolated axons. Initially, a total of 253 anterograde-directed fluorescent puncta were analyzed for mRFP or GFP fluorescence or if both fluorophores were present on the same migrating structure. Another 258 anterograde-moving, VP26-mRFP-positive structures were analyzed for detectable GFP content.

were equivalent for all three PRV strains, indicating similar production of infectious progeny (Fig. 1C). However, titers in the N compartment at this time were markedly different, depending on the PRV strain. PRV expressing wild-type Us9 spread efficiently to the N compartment, producing viral titers ranging between 10^7 and 10^8 PFU/ml. PRV 164, the mutant expressing Us9-GFP, spread poorly or not at all to the N compartment, as noted previously (20). In contrast, the PRV strain expressing the GFP-Us9 fusion protein (PRV 340) spread to the N compartment in all chambers, with viral titers near 10^7 PFU/ml, an approximately 1-log decrease from wild-type Us9 titers at the same time (Fig. 1C). The decrease in the N compartment titer of GFP-Us9 expressing PRV is not due to reduced viral amplification; wild-type-expressing and GFP-Us9-expressing PRV strains have equivalent replication kinetics in PK15 cells (Fig. 1D). We conclude that GFP-Us9 protein is functional for promoting significant anterograde spread of infection in our *in vitro* system.

Subcellular localization and transport of GFP-Us9. Since the new GFP-Us9 fusion protein was capable of supporting anterograde spread of PRV, we next determined the localization of GFP-Us9 in infected cells. Previously, Us9 and Us9-GFP have been characterized to accumulate in both the plasma membrane and intracellular puncta in infected cells (9, 10, 19, 23). We imaged superior cervical ganglion (SCG) neurons infected with a PRV strain expressing GFP-Us9 and VP26-monomeric red fluorescent protein (mRFP) (14) (PRV 341) late in infection to determine if GFP-Us9 had an altered localization compared to previous work. GFP-Us9 accumulated in both the soma and axonal plasma membrane (Fig. 2A). Further, GFP-Us9 localized to cytoplasmic punctate structures in the neuronal soma, some of which also contained VP26-mRFP puncta. We also found GFP-Us9 in punctate axonal structures associated with VP26-mRFP. We next imaged these structures, which may represent virions moving in the anterograde direction.

In the absence of Us9 protein or when the defective Us9-GFP fusion protein has been expressed, no viral capsids are found in axons of infected neurons (8). However, consecutive frames from a representative movie of GFP-Us9 and VP26-mRFP puncta show cotransport of the two viral fluorescent fusion proteins in the anterograde direction within axons (Fig. 2). As we previously observed, axons contain abundant GFP-Us9 puncta with a subset of these puncta colabeled with VP26-mRFP. In the selected frames, two VP26-mRFP structures are colabeled with GFP-Us9 and moving in the anterograde direction (Fig. 2B; see Movie S1 in the supplemental material). When we quantified axons for fluorescent structures moving in the anterograde direction, the majority of GFP-Us9 puncta, over 60%, did not colocalize with detectable VP26-mRFP puncta. When we looked exclusively at anterograde-directed VP26-mRFP positive puncta, 96.5% of these puncta were colabeled with GFP-Us9 (Fig. 2C). We conclude that the VP26-mRFP puncta are capsid assemblies that move in the anterograde direction only when complexed with GFP-Us9.

A mutant Us9 is not cotransported with anterograde-directed capsids. We next constructed a PRV recombinant expressing a previously characterized Us9 missense protein fused to the amino terminus of GFP. This mutant carries alanine substitution mutations in the conserved dityrosine motif located at the start of the acidic protein cluster in the cytoplasmic domain (Y49-50A). These residues are essential for Us9-mediated anterograde-directed viral spread of infection in a rat eye model (24). We tested

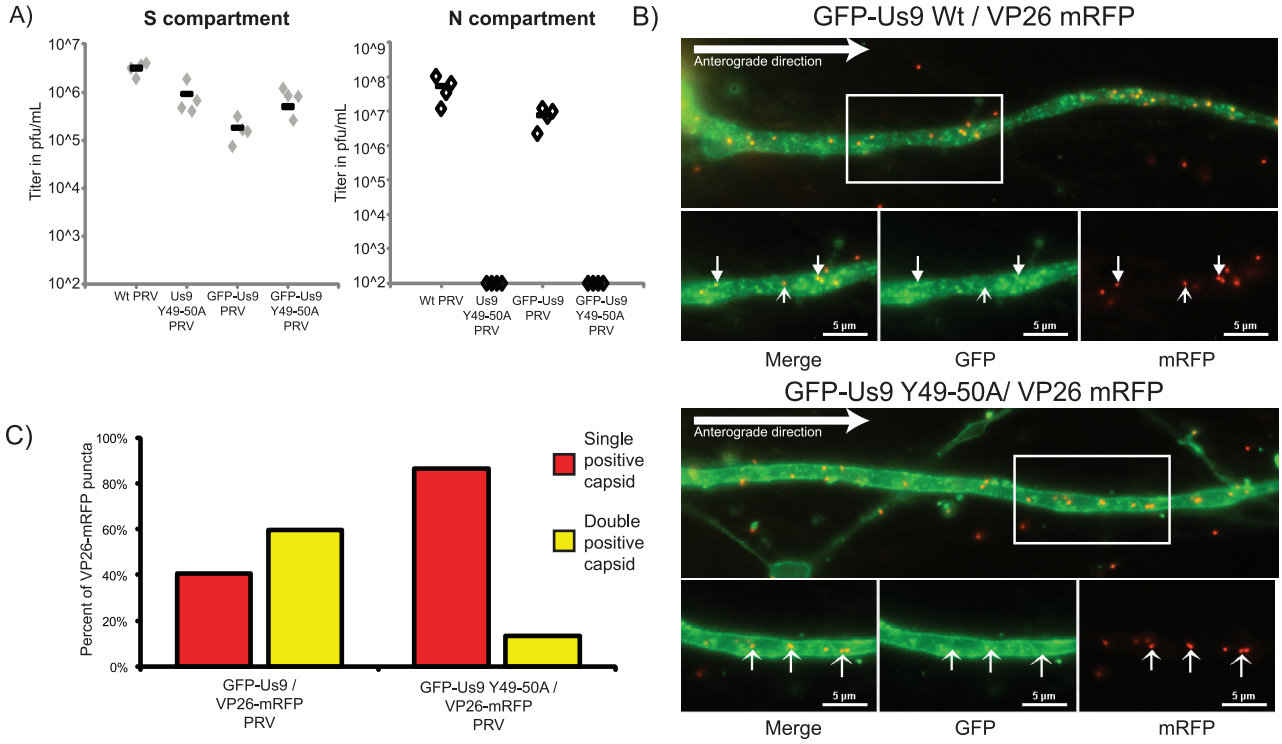

FIG 3 Us9 function is necessary for anterograde transport of capsids. (A) Analysis of anterograde transport capacity of PRV strains expressing mutated forms of Us9 or GFP-Us9. Viral titers of wild-type (Wt) Us9 (PRV 328), the Us9 Y49-50A mutant (PRV 172), GFP-Us9 (PRV 340), and the GFP-Us9 Y49-50A mutant (PRV 440) in the S and N compartments of compartmentalized neuronal cultures were determined at 24 h postinfection of the S compartment. (B) Representative images of SCG axons infected with either GFP-Us9/VP26-mRFP (PRV 341) or GFP-Us9 Y49-50A/VP26-mRFP (PRV 442) and fixed with 4% paraformaldehyde at 8 h postinfection. Closed arrowheads indicate doubly positive structures, whereas open arrowheads indicate singly positive structures. Scale bars, 5 μm. (C) Quantitation of dually and singly labeled VP26-mRFP puncta in SCG axons infected with PRV 341 or PRV 442. Quantitation was performed on 5 cells per infection and covered the initial 150 to 225 nm of the SCG axon. The numbers of doubly positive (yellow) and singly positive (red) VP26-mRFP puncta are expressed as percentages of the total structures counted across all of the images.

the anterograde spread capacity of PRV expressing GFP-Us9 Y49-50A (PRV 440) in the compartmentalized neuronal culture system (Fig. 3A). As predicted, PRV strains expressing either the native or the GFP-fused version of the dityrosine missense protein were completely incapable of supporting spread to the N compartment, confirming that these strains are defective in anterograde spread.

The anterograde spread deficiency phenotype observed with GFP-Us9 Y49-50A may be caused by either an inability of the missense protein to sort viral proteins into axons or an inability to engage anterograde transport machinery. To determine if virion transport in axons was blocked or reduced, we constructed PRV strains that expressed both the GFP-Us9 Y49-50A and VP26-mRFP fusion proteins (PRV 442) and infected dissociated SCG cultures as before. In axons of PRV 442-infected neurons, there were no anterograde-directed VP26-mRFP puncta compared to PRV 341 (wild-type GFP-Us9/VP26-mRFP)-infected neurons at comparable times after infection (see Movies S2 and S3 in the supplemental material). To quantify the numbers of colabeled virion structures, the cultures were fixed and VP26-mRFP puncta were counted (Fig. 3B). The number of colabeled puncta in PRV 442-infected axons was markedly lower than that of those found after comparable PRV 341 infection (Fig. 3C). We suspect that the small numbers of dually labeled structures observed in PRV 442 infections are similar to immobile dually labeled structures in the movies in the supplemental material. Interestingly, while VP26-mRFP puncta were not moving in the anterograde direction after PRV 442 infection, substantial numbers of singly labeled GFP-Us9 Y49-50A puncta continued to move in the anterograde direction. This observation suggests that while the dityrosine motif in Us9 is essential to promote efficient sorting and transport of VP26-mRFP puncta (presumably capsids), it has little to no effect on the capacity of the mutant Us9 fusion protein itself to enter and move in axons.

GFP-Us9 is cotransported with other viral membrane proteins. To determine if the GFP-Us9 puncta not associated with VP26-mRFP contain other viral membrane proteins, we fused mCherry to the carboxy terminus of PRV gM, a conserved glycoprotein present in viral and cellular membranes with known involvement in secondary envelopment (25, 26). The gM-mCherry fusion protein replaced endogenous gM and was expressed from the endogenous gM promoter. We imaged dissociated SCG neurons infected with a double-recombinant virus expressing both GFP-Us9 and gM-mCherry (PRV 348). At distal axon sites, many doubly positive punctate structures were observed moving in the anterograde direction (Fig. 4; see Movie S4 in the supplemental material), 96% of the GFP-Us9-positive structures moving in the anterograde direction were also positive for gM-mCherry. Conversely, very few structures were singly labeled with GFP-Us9 or gM-mCherry. The high concordant localization of these two viral

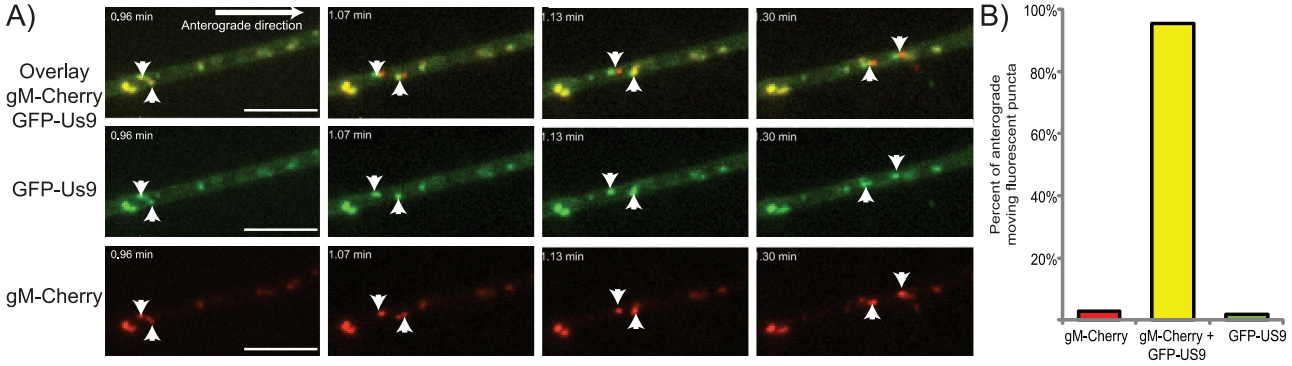

FIG 4 GFP-Us9 and gM-mCherry are cotransported in axonal anterograde-directed structures. (A) Representative images from Movie S3 in the supplemental material with GFP-Us9, gM-mCherry, and an overlay of the two fluorescence channels displayed as indicated. PRV 348 was used to infect dissociated SCG cultures. At 6 To 8 h postinfection, distal axon sites were imaged by epifluorescence microscopy. Scale bars, 5 μm. (B) Quantitation of eight movies was performed where anterograde-directed viral structures were scored for visible labeling with GFP-Us9, gM-mCherry, or both. A total of 214 anterograde-directed punctate structures were counted, the majority of which were colabeled with visible amounts of GFP-Us9 and gM-mCherry.

membrane proteins suggests that they are alternative products of virion production which could include light particles or vesicles carrying viral membrane proteins only (Fig. 5). The full composition of these structures and their role in anterograde viral spread remain to be resolved.

DISCUSSION

Viral protein Us9 is essential for anterograde-directed spread of PRV infection *in vitro* and *in vivo*. Our goal was to visualize the transport dynamics, localization, and function of PRV Us9 by using fluorescent fusion proteins and live-cell imaging of infected neurons. We could not use a previously characterized carboxy-terminal fusion of GFP to Us9 (Us9-GFP) because it was defective for anterograde-directed spread of infection. However, we characterized an N-terminal fusion (GFP-Us9) and found that it retains the ability to promote anterograde spread of PRV. GFP-Us9 was associated with anterograde moving viral particles (labeled with VP26-mRFP or gM-mCherry). A GFP-Us9 missense mutant incapable of anterograde spread (Y49-50A) did not sponsor anterograde-directed capsids, but the missense fusion protein itself moved into axons and was transported in the anterograde direction. These fluorescent viral fusion proteins have allowed the visualization of viral processes associated with the directed spread of infection in neurons.

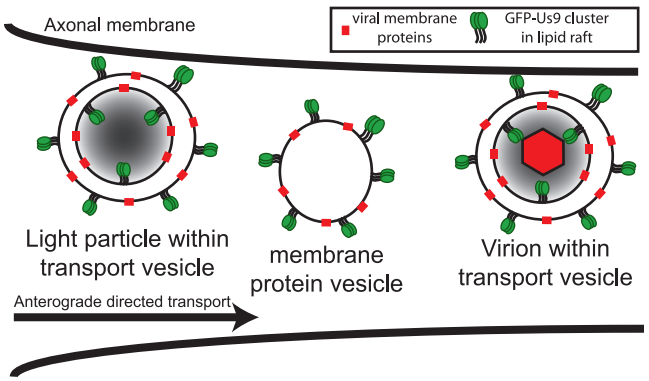

FIG 5 Schematic model of Us9 incorporation into viral particles. Three classes of viral particles are potentially labeled with GFP-Us9 as they undergo anterograde-directed transport within the axon: virions containing capsid assemblies, viral membrane proteins, and GFP-Us9. Subvirion assemblies that lack capsids but contain tegument proteins known as light particles would also associate with GFP-Us9. Finally, intracellular membranes containing viral membrane proteins (membrane protein vesicles) that would topologically resemble secretory vesicles would also be marked by GFP-Us9.

Our data are in concordance with the married model of PRV transport: fully assembled virions, enclosed in a membranous transport vesicle, are transported in axons in an anterograde direction. This model has been validated using a variety of experimental techniques for PRV, including fluorescent and electron microscopy coupled with compartmentalized neuronal culturing (12, 13). The significant coassociation of GFP-Us9 with almost all anterograde-directed capsids is greater than results reported for other viral membrane proteins (12, 27). In contrast, the structures being transported during HSV infection remain controversial (16, 17, 27–30). There are conflicting reports about the role of Us9 in HSV spread (31, 32) and that Us9 does not associate with HSV membrane proteins (33). The development of a functional HSV GFP-Us9 fusion may help resolve the disparate observations and models for HSV transport.

Intracellular membrane localization of Us9 is important for sorting newly assembled virions from the cell body into axons. Us9 in lipid rafts is essential for axonal sorting and anterograde spread of infection but not for incorporation into virion membranes or for virion egress from the cell bodies of neurons (18). Us9 is predicted to localize within the membranes of the virion transport vesicle such that the functional domains of Us9 are exposed to the intracellular environment. This would allow Us9 to directly engage proteins that are required for axonal sorting and anterograde transport of vesicles containing virions (9, 34). Us9 is incorporated into the virion envelope (11, 35), but the GFP-Us9 labeling of extracellular virions is at or below the limit of detection under optical conditions identical to those used in this study (unpublished results). This raises the possibility that the concentration of GFP-Us9 within virions is variable and reduced compared to that of intracellular virions surrounded by a transport vesicle membrane. The fact that we can observe GFP-Us9 as fluorescent puncta associated with capsids in axons suggests that Us9 may be preferentially incorporated into the membrane of the intracellular transport vesicle surrounding virions rather than virion enve-

lopes. Regulation of Us9 activity may also occur by posttranslational modifications such as phosphorylation (11). However, a simple model is that differential incorporation of GFP-Us9 into transport vesicles could regulate whether or not virions are sorted into axons. Vesicles with lower GFP-Us9 activity would egress from the cell body, while vesicles with increased GFP-Us9 activity would be sorted into axons.

The number of GFP-Us9 puncta without capsids moving in the anterograde direction is striking, with over 60% of the total fluorescently labeled puncta lacking a detectable VP26-mRFP signal. The coassociation of wild-type GFP-Us9 with gM-mCherry in almost all anterograde-trafficking particles suggests that viral membrane protein assemblies are involved. These structures might include capsid-less light particles (36), as well as vesicle precursors involved in virion formation (Fig. 5). The relevance and impact of nonvirion structures on the spread of infection remain to be determined. While the number of structures observed might be influenced by *in vitro* culture conditions, light particle production does occur *in vivo* (37). Interestingly, the GFP-Us9 missense mutant Y49-50A moves efficiently in the anterograde direction in the absence of full virions. It is possible that membrane-associated Us9 facilitates transport for any vesicular membrane, and the Y49-50A mutation alters a second function involved in the recruitment of mature virions into axons. Alternatively, the Y49-50A mutant may be incorporated into membranes and passively carried along a cellular secretion pathway. Further experimentation is required to understand the nature and importance of these nonvirion structures.

One caveat of our study is that the GFP-Us9 fusion protein does not completely restore viral spread to wild-type levels. Further observation of viral transport and spread using different mutant Us9 proteins will allow us characterize the modest deficiency related to the GFP fusion, as well as to dissect Us9 function.

In conclusion, this fluorescent fusion protein enables us, for the first time, to visualize Us9-dependent axonal sorting events. Further goals of studies utilizing this functional fusion protein include the identification of protein interaction partners, understanding of the functional defects of Us9 point mutations, and testing of the model of differential Us9 incorporation into a subset of viral membranes. GFP-Us9 is an important reagent leading to the eventual understanding of Us9's function in alphaherpesvirus spread and disease.

MATERIALS AND METHODS

Plasmids and viruses. The PRV mutant expressing GFP-Us9 (PRV 340) was constructed by cloning the PRV Us9 opening reading frame into the EcoRI site of pEGFP-C1. A flexible hydrophilic linker was placed between the GFP moiety and the Us9 protein (38); the nucleotide sequence of the linker region was 5′ GAAT*TC*GCCCTTCGGAGAAGGACAAGGACAAG *GACAAGGACCCGGAAGAGGATATGCCTATAGAAGT* 3′ (the EcoRI site is underlined, and the linker sequence is italicized), which translated into the peptide sequence SPFGEGQGQGQGPGRGYAYRS. The plasmid construct was designated pML122. In order to recombine pML122 into the gG locus of the PRV genome, 3 to 4 μg of plasmid was digested with NsiI, heat inactivated at 80°C for 20 min, and transfected into 293T cells (~10^7 cells per 10-cm dish) using Lipofectamine 2000 and following the manufacturer's instructions (Invitrogen, Carlsbad, CA). At 2 h posttra nsfection, cells were infected with PRV 337 (19) and incubated until a significant cytopathic effect (CPE) was observed, approximately 48 h pos ttransfection. Targeted homologous recombination between pML122 and PRV 337 was predicted to occur between the 5′ homologous arm of the NsiI fragment containing the cytomegalovirus promoter and the 3′ homologous arm containing sequence downstream of the simian virus 40 poly(A) site. Cells and medium were then collected together, serially dilu ted, and plated onto PK15 cells. Individual plaques expressing GFP-Us9 were identified using a Nikon Eclipse TE300 inverted epifluorescence mi croscope. Initial isolates were subjected to three further rounds of plaque purification and examined by Western blot analysis to confirm the expression of PRV GFP-Us9 and the loss of expression of bovine herpesvirus Us9. This virus strain was designated PRV 340. The construction of GFP-Us9 Y49-50A was done in a similar manner using *de novo* synthesis methods to generate Us9 with alanine codon substitutions at tyrosines 49 and 50 (24) also containing the flexible linker sequence. This construct was cloned into pEGFP-C1 as described above, which was then used to generate a PRV strain expressing GFP-Us9 Y49-50, designated PRV 440. To construct the recombinant PRV strain expressing GFP-Us9 and VP26-mRFP (14), PK15 cells were coinfected at a multiplicity of infection (MOI) of 10 PFU per cell with 1×10^7 PFU of PRV 340 and PRV 325 (Us9-null/VP26-mRFP virus isolated as described in reference 8) and allowed to undergo full CPE; the isolated virus was designated PRV 337. Individual fluorescent plaques expressing both GFP and mRFP were isol ated and purified for three subsequent rounds of plaque purification as described above and designated PRV 341. Coinfection of PRV 440 and PRV 325 was also used to isolate GFP-Us9 Y49-50A/VP26-mRFP, design ated PRV 442.

A PRV recombinant expressing a gM-mCherry fusion protein was constructed by *de novo* synthesis (GenScript USA Inc., Piscataway, NJ.) of a plasmid containing the terminal 500 bp of the UL10 open reading frame (gM) with an in-frame fusion of mCherry fluorescent protein and 500 bp of downstream flanking sequence. This plasmid was linearized by EcoRI and SalI restriction enzyme digestion and directly cotransfected with PRV Becker nucleocapsid DNA. Virus was harvested, and limiting dilutions were made to isolate individual plaques on PK15 cells. Individual plaques expressing gM-mCherry were identified using a Nikon Eclipse TE300 inverted epifluorescence microscope. These initial isolates were subjected to three subsequent rounds of plaque purification to generate PRV 347. To isolate a virus expressing gM-mCherry and GFP-Us9, gM-Cherry plasmid DNA was linearized and cotransfected with PRV 340 nucleocapsid DNA. Doubly positive gM-mCherry- and GFP-Us9-expressing plaques were isolated and subjected to three rounds of plaque purification. This virus was designated PRV 348.

Neuronal culturing and infection. PK15 cells were maintained in 10% fetal bovine serum (FBS)-1% penicillin-streptomycin in Dulbecco's modified Eagle's medium (DMEM). Primary neuronal cultures of SCG neurons were maintained in neuronal medium, which consists of Neurobasal medium (Invitrogen, Carlsbad, CA) supplemented with 1% penicillin-streptomycin-glutamine (Invitrogen), B27 Supplement (Invitrogen), and 50 ng/ml neuronal growth factor 2.5 S (Invitrogen). Prior to neuron plating, cell culture surfaces were coated with polyornithine (Sigma-Aldrich, St. Louis, MO) at 500 μg/ml in borate buffer, pH 8.2, followed by murine laminin (Invitrogen) at 10 μg/ml in calcium- and magnesium-free Hanks balanced salt solution. Compartmentalized neuronal cultures were prepared as described in references 13 and 39. Briefly, plastic tissue culture dishes were treated as described above and air dried. Parallel grooves were etched into the surface, and a 1% methylcellulose–1× DMEM solution was spotted onto the grooves. CAMP320 Teflon isolator rings (Tyler Research; Edmonton, Alberta, Canada) were coated with autoclaved vacuum grease on one side and gently applied to the treated culture surface such that the parallel grooves extended across the three compartments. The compartments were individually filled with neuronal medium and tested for leaks. Dissociated SCG neurons were plated into one side (S) compartment. Cultures were maintained until axon extensions had robustly penetrated and grown into the far-side (N) compartment, typically 17 to 21 days after dissociation.

Viral infections of PK15 cells were performed in 2% FBS-containing medium. Viral titer determination was similar to infection, but the me-

dium was supplemented with 1% methylcellulose to limit virus diffusion. Three days postinfection, methylcellulose medium was aspirated and cells were stained with methylene blue solution to visualize the cell monolayer.

For infection of dissociated or compartmentalized SCG neuronal cultures, approximately 1×10^6 PFU of virus was used per dish, diluted in 100 to 200 μl of conditioned neuronal medium. SCG neurons were not infected until 17 to 24 days of culturing to allow full neuronal maturation. Infection of compartmentalized neurons and quantitation of virions that have undergone anterograde-directed transport require specific preparations. One day prior to infection, approximately 5×10^5 PK15 cells in 1% FBS-supplemented neuronal medium are plated on top of the isolated axons in the N compartment (Fig. 1B). The cells amplify anterograde-spreading virions in the N compartment, enhancing the detection of spread events. Prior to the application of viral inoculum to the S compartment, 1% methylcellulose-supplemented neuronal medium is placed within the middle compartment. Though silicone grease is sufficient to seal and isolate the compartments, the methylcellulose prevents accidental viral diffusion between the compartments in the unlikely event that the grease barrier is compromised.

Imaging. Fluorescent particles were imaged in dissociated SCG cultures on a MatTek glass bottom dish (MatTek Corporation, Ashland, MA). Infections were performed as described above. Epifluorescence imaging was performed on a Nikon Ti-Eclipse inverted microscope equipped with separate fast-switching excitation and emission filter wheels (Prior Scientific, Rockland, MA). This system allowed rapid serial acquisition of multiple fluorescence channels. The microscope is also equipped with a heated cell culture chamber (Ibidi; Martinsried, Germany) to ensure biologically relevant environmental conditions during image acquisition. Images were acquired with either a CoolSnap ES2 charge-coupled device (CCD) camera (Photometrics, Tucson, AZ) or an Ixon 895 back-thinned EM-CCD camera (Andor; Belfast, Northern Ireland). All images were acquired with a 100× Plan Apo VC objective (Nikon Instruments, Melville, NY) with differential interference contrast optics. Live movies were obtained using NIS-Elements ND acquisition, resulting in the sequential acquisition of two fluorescence channels at a maximum acquisition frequency of one frame every 0.9 s. Supplemental movies were converted into. AVI files using NIS-Elements.

ACKNOWLEDGMENTS

We appreciate the guidance and critical commentary of all of the members of the Enquist laboratory.

L.W.E. and R.K. are supported by U.S. National Institutes of Health grants R37 NS033506-16 and R01 NS060699-03. M.P.T. is supported by an American Cancer Society postdoctoral research fellowship (PF-10-057-01-MPC). T.K. is supported by a National Science Foundation graduate research fellowship (DGE-0646086). M.G.L. was supported by an American Cancer Society Eastern Division Mercer Board postdoctoral fellowship (PF-08-264-01-MBC).

SUPPLEMENTAL MATERIAL

Supplemental material for this article may be found at http://mbio.asm.org/lookup/suppl/doi:10.1128/mBio.00063-12/-/DCSupplemental.

Movie S1, AVI file, 1 MB.
Movie S2, AVI file, 3.1 MB.
Movie S3, AVI file, 3.4 MB.
Movie S4, AVI file, 4.2 MB.

REFERENCES

1. **Koelle DM, Corey L.** 2008. Herpes simplex: insights on pathogenesis and possible vaccines. Annu. Rev. Med. 59:381–395..
2. **Steiner I, Kennedy PGE, Pachner AR.** 2007. The neurotropic herpes viruses: herpes simplex and varicella-zoster. Lancet Neurol. **6**:1015–1028.
3. **Enquist LW, Tomishima MJ, Gross S, Smith GA.** 2002. Directional spread of an alpha-herpesvirus in the nervous system. Vet. Microbiol. **86**:5–16.
4. **Pomeranz LE, Reynolds AE, Hengartner CJ.** 2005. Molecular biology of pseudorabies virus: impact on neurovirology and veterinary medicine. Microbiol. Mol. Biol. Rev. **69**:462–500.
5. **Brideau AD, Card JP, Enquist LW.** 2000. Role of pseudorabies virus Us9, a type II membrane protein, in infection of tissue culture cells and the rat nervous system. J. Virol. **74**:834–845.
6. **Card JP, Whealy ME, Robbins AK, Moore RY, Enquist LW.** 1991. Two alpha-herpesvirus strains are transported differentially in the rodent visual system. Neuron **6**:957–969.
7. **Kimman TG, et al.** 1992. Role of different genes in the virulence and pathogenesis of Aujeszky's disease virus. Vet. Microbiol. **33**:45–52.
8. **Lyman MG, Feierbach B, Curanovic D, Bisher M, Enquist LW.** 2007. Pseudorabies virus us9 directs axonal sorting of viral capsids. J. Virol. **81**:11363–11371.
9. **Tomishima MJ, Enquist LW.** 2001. A conserved alpha-herpesvirus protein necessary for axonal localization of viral membrane proteins. J. Cell Biol. **154**:741–752.
10. **Brideau AD, Banfield BW, Enquist LW.** 1998. The Us9 gene product of pseudorabies virus, an alphaherpesvirus, is a phosphorylated, tail-anchored type II membrane protein. J. Virol. **72**:4560–4570.
11. **Brideau AD, del Rio T, Wolffe EJ, Enquist LW.** 1999. Intracellular trafficking and localization of the pseudorabies virus Us9 type II envelope protein to host and viral membranes. J. Virol. **73**:4372–4384.
12. **Antinone SE, Smith GA.** 2006. Two modes of herpesvirus trafficking in neurons: membrane acquisition directs motion. J. Virol. **80**:11235–11240.
13. **Ch'ng TH, Enquist LW.** 2005. Neuron-to-cell spread of pseudorabies virus in a compartmented neuronal culture system. J. Virol. **79**:10875–10889.
14. **del Rio T, Ch'ng TH, Flood EA, Gross SP, Enquist LW.** 2005. Heterogeneity of a fluorescent tegument component in single pseudorabies virus virions and enveloped axonal assemblies. J. Virol. **79**:3903–3919.
15. **Feierbach B, Bisher M, Goodhouse J, Enquist LW.** 2007. *In vitro* analysis of transneuronal spread of an alphaherpesvirus infection in peripheral nervous system neurons. J. Virol. **81**:6846–6857.
16. **Huang J, Lazear HM, Friedman HM.** 2011. Completely assembled virus particles detected by transmission electron microscopy in proximal and mid-axons of neurons infected with herpes simplex virus type 1, herpes simplex virus type 2 and pseudorabies virus. Virology **409**:12–16.
17. **Maresch C, et al.** 2010. Ultrastructural analysis of virion formation and anterograde intraaxonal transport of the alphaherpesvirus pseudorabies virus in primary neurons. J. Virol. **84**:5528–5539.
18. **Lyman MG, Curanovic D, Enquist LW.** 2008. Targeting of pseudorabies virus structural proteins to axons requires association of the viral Us9 protein with lipid rafts. PLoS Pathog. **4**:e1000065.
19. **Lyman MG, Kemp CD, Taylor MP, Enquist LW.** 2009. Comparison of the pseudorabies virus Us9 protein with homologs from other veterinary and human alphaherpesviruses. J. Virol. **83**:6978–6986.
20. **Lyman MG, Curanovic D, Brideau AD, Enquist LW.** 2008. Fusion of enhanced green fluorescent protein to the pseudorabies virus axonal sorting protein Us9 blocks anterograde spread of infection in mammalian neurons. J. Virol. **82**:10308–10311.
21. **Campenot RB.** 1977. Local control of neurite development by nerve growth factor. Proc. Natl. Acad. Sci. U. S. A. **74**:4516–4519.
22. **Campenot RB, Lund K, Mok SA.** 2009. Production of compartmented cultures of rat sympathetic neurons. Nat. Protoc. **4**:1869–1887.
23. **Ch'ng TH, Enquist LW.** 2005. Efficient axonal localization of alphaherpesvirus structural proteins in cultured sympathetic neurons requires viral glycoprotein E. J. Virol. **79**:8835–8846.
24. **Brideau AD, Eldridge MG, Enquist LW.** 2000. Directional transneuronal infection by pseudorabies virus is dependent on an acidic internalization motif in the Us9 cytoplasmic tail. J. Virol. **74**:4549–4561.
25. **Crump CM, et al.** 2004. Alphaherpesvirus glycoprotein M causes the relocalization of plasma membrane proteins. J. Gen. Virol. **85**:3517–3527.
26. **Kopp M, Granzow H, Fuchs W, Klupp B, Mettenleiter TC.** 2004. Simultaneous deletion of pseudorabies virus tegument protein UL11 and glycoprotein M severely impairs secondary envelopment. J. Virol. **78**:3024–3034.
27. **Wisner TW, Sugimoto K, Howard PW, Kawaguchi Y, Johnson DC.** 2011. Anterograde transport of herpes simplex virus capsids in neurons by both separate and married mechanisms. J. Virol. **85**:5919–5928.
28. **Antinone SE, Zaichick SV, Smith GA.** 2010. Resolving the assembly state of herpes simplex virus during axon transport by live-cell imaging. J. Virol. **84**:13019–13030.

29. **Ibiricu I, et al.** 2011. Cryo electron tomography of herpes simplex virus during axonal transport and secondary envelopment in primary neurons. PLoS Pathog. **7**:e1002406.
30. **Negatsch A, et al.** 2010. Ultrastructural analysis of virion formation and intraaxonal transport of herpes simplex virus type 1 in primary rat neurons. J. Virol. **84**:13031–13035.
31. **Lavail JH, Tauscher AN, Sucher A, Harrabi O, Brandimarti R.** 2007. Viral regulation of the long distance axonal transport of herpes simplex virus nucleocapsid. Neuroscience **146**:974–985.
32. **McGraw HM, Awasthi S, Wojcechowskyj JA, Friedman HM.** 2009. Anterograde spread of herpes simplex virus type 1 requires glycoprotein E and glycoprotein I but not Us9. J. Virol. **83**:8315–8326.
33. **Snyder A, Polcicova K, Johnson DC.** 2008. Herpes simplex virus gE/gI and US9 proteins promote transport of both capsids and virion glycoproteins in neuronal axons. J. Virol. **82**:10613–10624.
34. **Tomishima MJ, Smith GA, Enquist LW.** 2001. Sorting and transport of alpha herpesviruses in axons. Traffic **2**:429–436.
35. **Kramer T, Greco TM, Enquist LW, Cristea IM.** 2011. Proteomic characterization of pseudorabies virus extracellular virions. J. Virol. **85**: 6427–6441.
36. **Szilágyi JF, Cunningham C.** 1991. Identification and characterization of a novel non-infectious herpes simplex virus-related particle. J. Gen. Virol. **72**:661–668.
37. **Alemañ N, et al.** 2003. L-particle production during primary replication of pseudorabies virus in the nasal mucosa of swine. J. Virol. **77**:5657–5667.
38. **Leonhardt H, et al.** 2000. Dynamics of DNA replication factories in living cells. J. Cell Biol. **149**:271–280.
39. **Curanovic D, Ch'ng TH, Szpara M, Enquist L.** 2009. Compartmented neuron cultures for directional infection by alpha herpesviruses. Curr. Protoc. Cell Biol. **Chapter 26:**Unit 26.4.